Supplemental Materials

Contents

1 Supplemental Movies

Supplemental Movie 1: Protocol for GVA sample embedding. weblink

Supplemental Movie 2: Live cell imaging of CellROX stained cells imaged under agarose pad with different concentrations of DPI. Pad is made with PMM. Time (HH:MM) annotated in the upper left. DPI was added on top of pad at start of video. weblink

2 Supplemental Tables

Supplemental Table 1: Pricing for viability measurement consumables and Spiral Plater instrumentation. weblink

3 Supplemental Figures

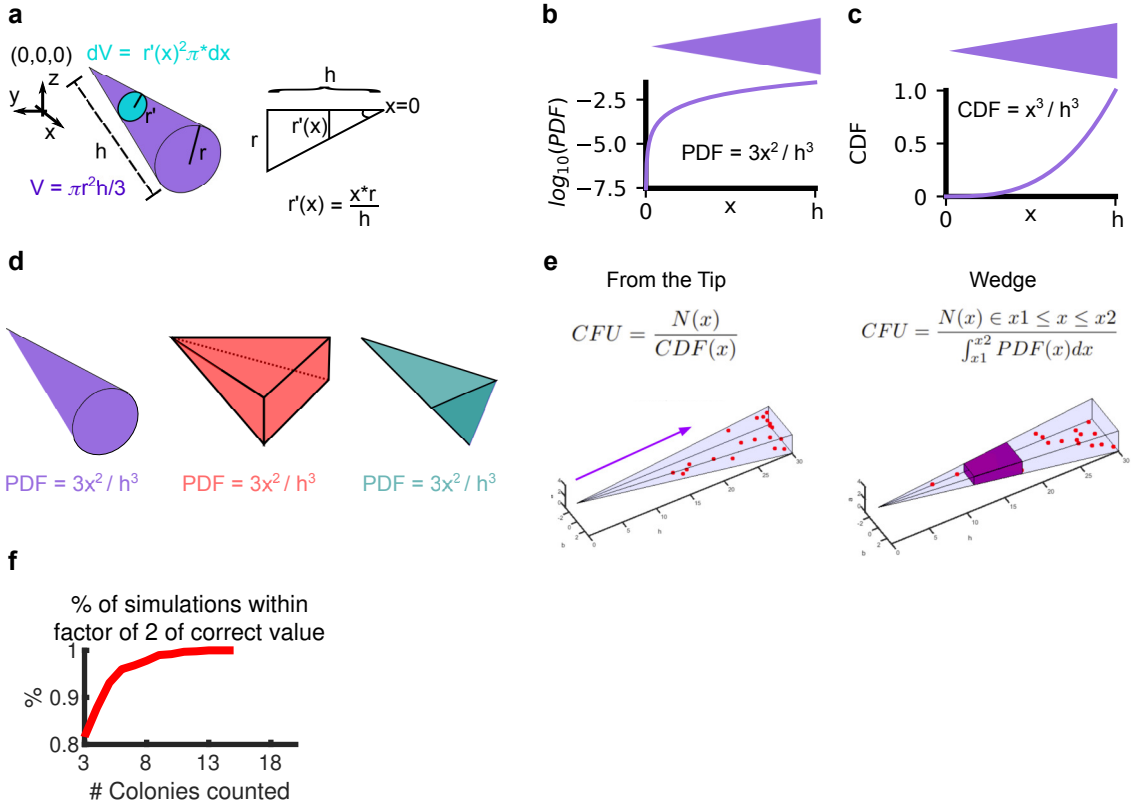

Figure S1: **Derivation of a cone's PDF.** a) The volume of the infinitesimal dV divided by the total volume V corresponds to the probability of finding a colony as a function of x. The radius of the infinitesimal ($r'(x)$) is a function of the radius of the cone's base (r) divided by the height of the cone (h) times x according to trigonometry. b) The PDF of the cone as a function of x. Overhead projection of cone is depicted above. c) The cumulative density function (CDF) as a function of x. d) The PDF is the same for axially symmetric cones such as a square (red) and triangle (turquoise) pyramids. e) Two equivalent ways of calculating the number of CFUs in the wedge using either the CDF (left) or PDF (right). $N(x)$ is the number of colonies counted. f) Percentage of simulations with the GVA calculated CFUs/mL within a factor of 2 of the correct value as a function of the number of colonies used for the GVA calculation. 1000 simulations used to calculate percentage. See Figure 1c for simulation parameters.

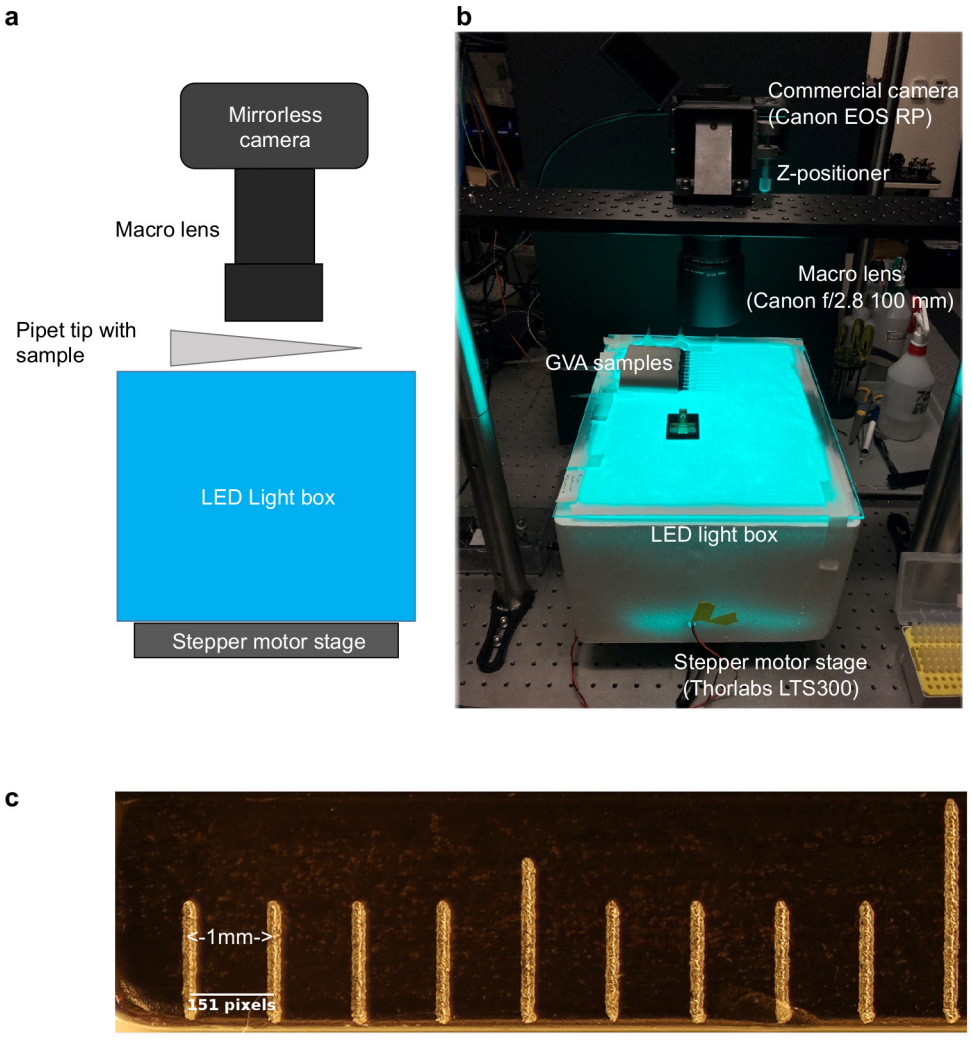

Figure S2: **Optical configuration.** a) Schematic of optical configuration for imaging the pipette tips containing agarose. A mirrorless camera with a macro lens is positioned above the tips at the focal plane. Addition of a z-positioner stage helps in fine tuning the focus. Pipettes are illuminated transversely using an LED light box with a diffuser. This box is mounted on a stepper motor to allow for imaging 12 pipettes at a time. The stepper motor and the camera are simultaneously controlled via LabView software. b) Picture of optical configuration. A cyan light was used to maximize the contrast of the TTC counterstain. A styrofoam box functions as a reflective light box and a sheet of paper as a diffuser. The GVA samples are positioned using a 12 channel pipetter and imaged using a Canon EOS RP camera with a f/2.8 100mm macro lens. c) Pixel resolution for this configuration is 6.7 microns.

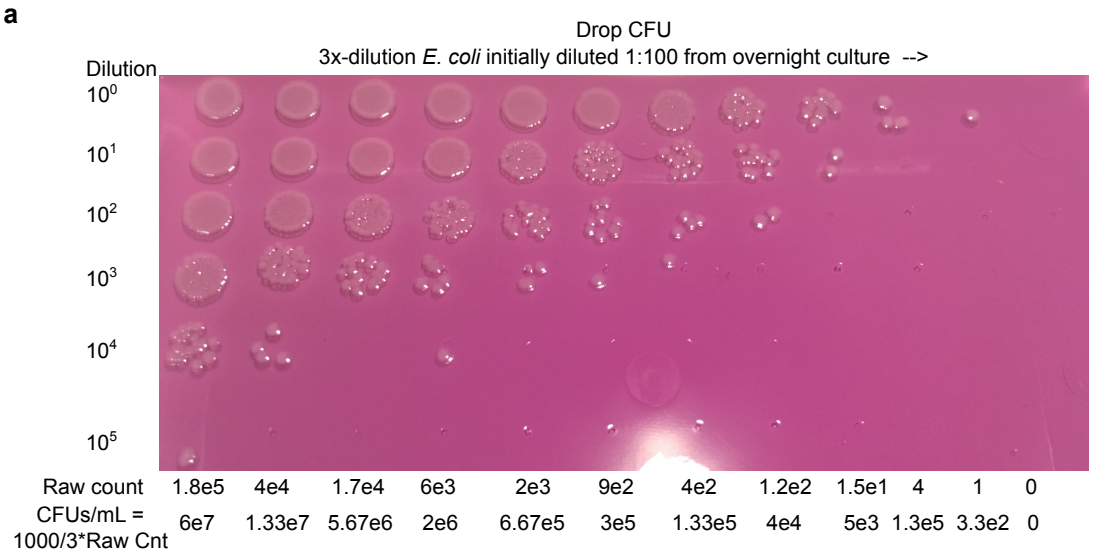

Figure S3: **Example drop CFU plate.** a) Each condition (columns) is diluted with a 10-fold serial dilution (rows) and 3uL are spotted on a 1.5% LB agar pad poured into an empty tip box. Colonies are counted for the dilution row where individual colonies are discrete. These counts are used to calculate the CFUs/mL (bottom).

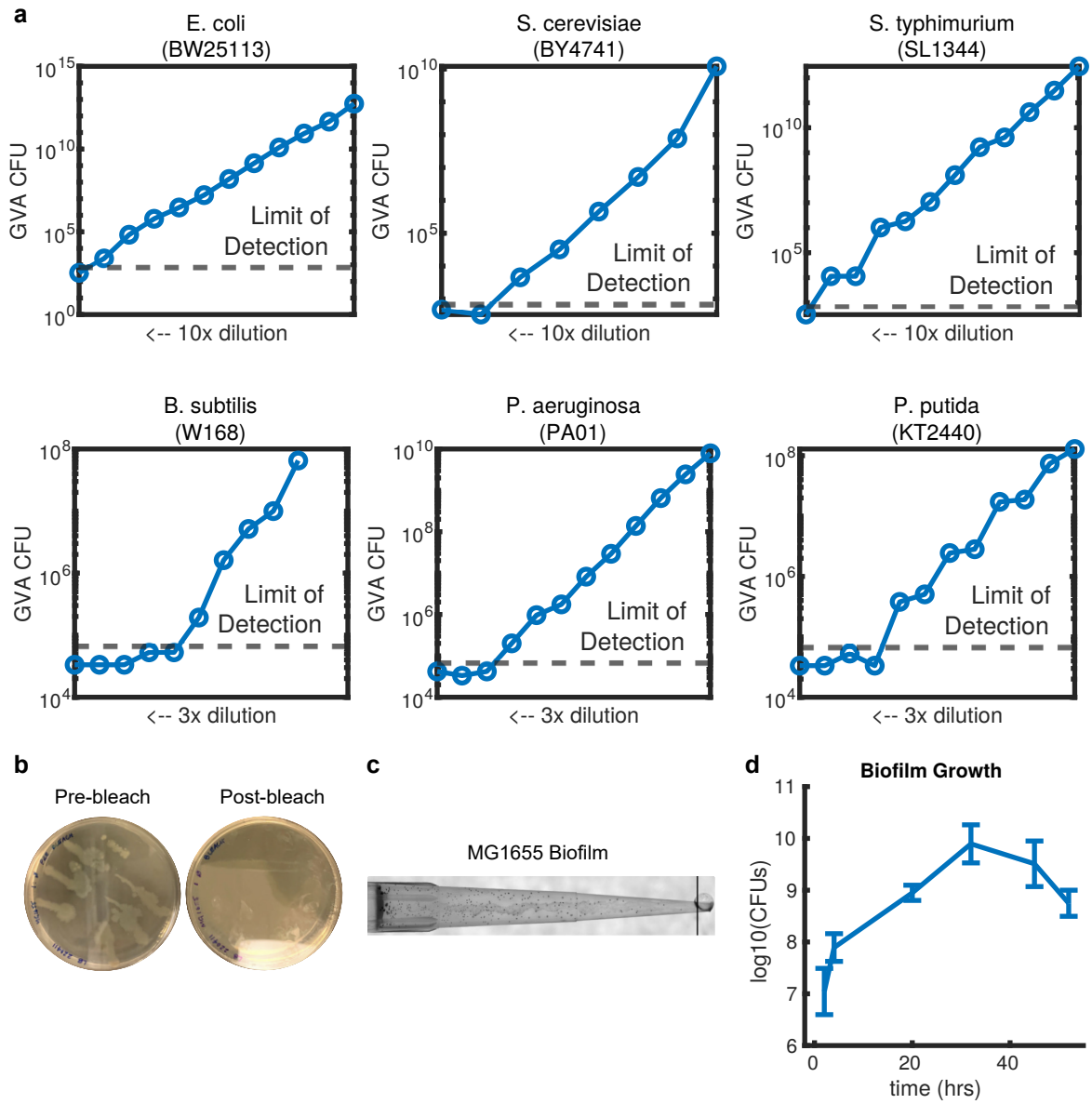

Figure S4: **GVA calculations for different species.** a) For the six species tested with GVA, the estimated number of CFUs/mL for different dilution series. b) Plates streaked with pipette tip after GVA embedding before or after bleach wash. No change in CFUs/mL were observed after bleach wash. c) Example GVA pipette tip for an *E. coli* biofilm. See Methods for culture and dissociation protocol. d) Biofilm growth over time. Errorbars correspond to standard deviation between ≥ 5 biological replicates.

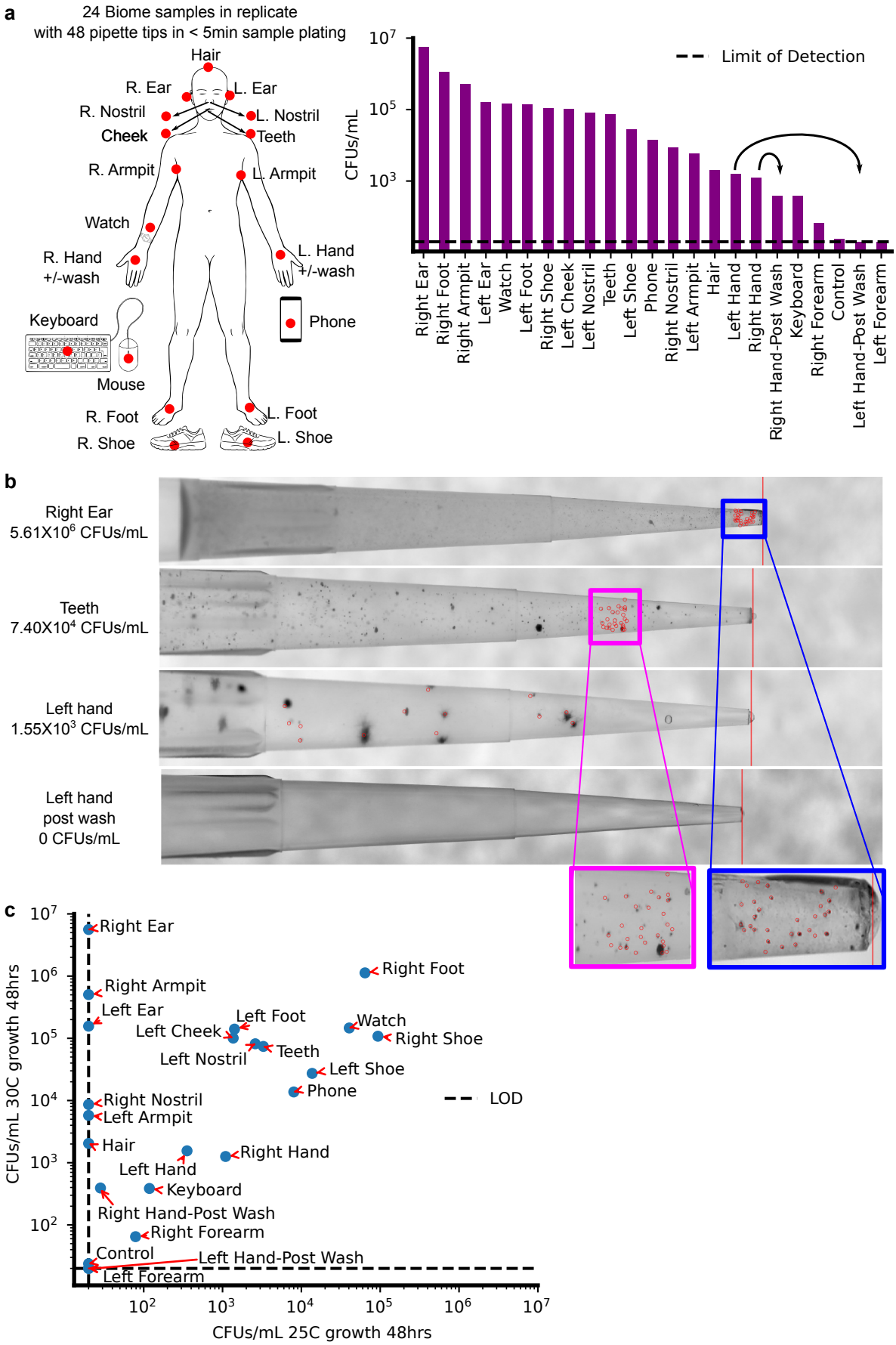

Figure S5: **Biome sampling using GVA.** a) Twenty-four positions (red dots) on a volunteer were swabbed vigorously for 15 seconds before being placed in 1 mL of LB medium and vortexed for 10 seconds. 50 μL of the sample was then mixed with 150 μL of 0.66% melted LB agar to a final concentration of 0.5% agar and allowed to gel in the tips. With this protocol, the lower limit of detection was 20 CFUs/mL (dotted line). The sample replicates were incubated at 30°C or 25°C for 48 hours before imaging. b) Example pipette tips for different sample regions reveals diverse colony structure and concentration for different biome locations. All samples were stained with TTC. c) Samples from higher thermal regions (ear, armpit) grew at 30°C but did not grow at 25°C indicating the temperature selectivity of different species grown in the pipette tip.

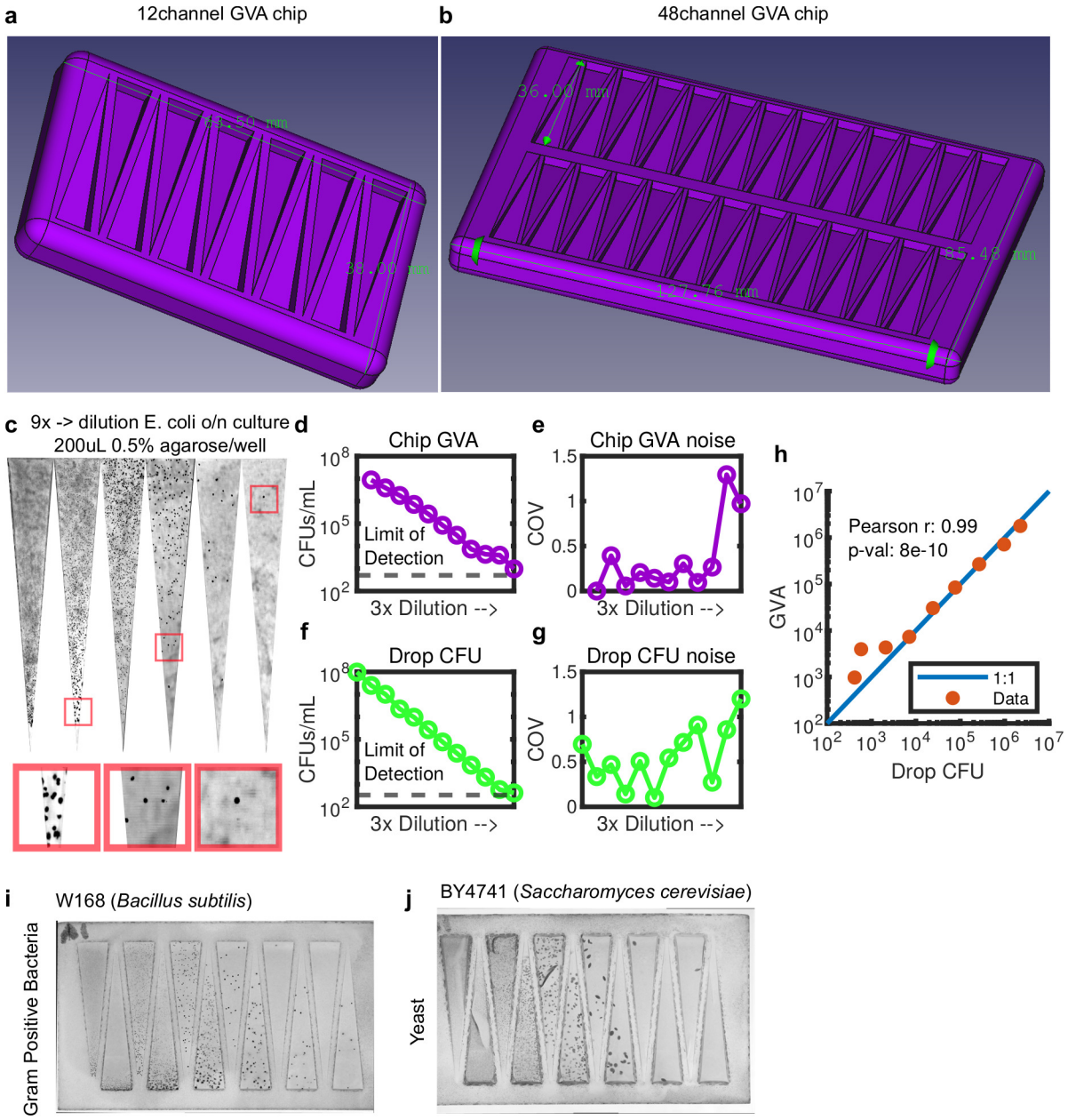

Figure S6: **Chip version of GVA uses the square pyramid geometry.** a,b) 3D printed molds for creating square pyramid for 12 (a) and 48 (b) conditions. c) Picture of a 9x dilution series of *E. coli* cultures on the GVA chip. d) GVA calculated CFUs/mL using for a dilution series. Each dot is the mean of 4 replicates. e) The noise, measured using the coefficient of variation (COV) for the chip GVA. f) Matched drop CFU quantification to conditions in (d). g) Corresponding noise analysis for drop CFU. h) Correlation between chip GVA and drop CFU over 5 orders of magnitude. i,j) Chip GVA for gram-positive (i) and eukaryotic (j) cells.

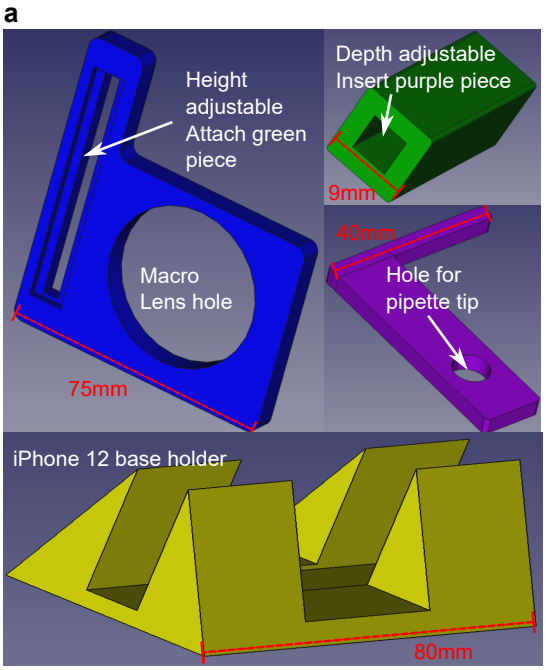

Figure S7: **iPhone pipette tip holder.** a) The 3D printed parts for stereotypically positioning a pipette tip in front of an iPhone rear camera with a Xenvo macro lens (15x magnification without the widefield lens). The blue face plate slides onto the Xenvo macro lens which is clipped to the iPhone. The green bar is attached with a screw to the side channel on the blue plate. This allows for adjusting the height by sliding the green bar in the channel. The purple extension bar slides into the green channel to adjust the imaging depth. Phone is held upright with stand (yellow). Pieces printed with standard FDM printing with PLA.

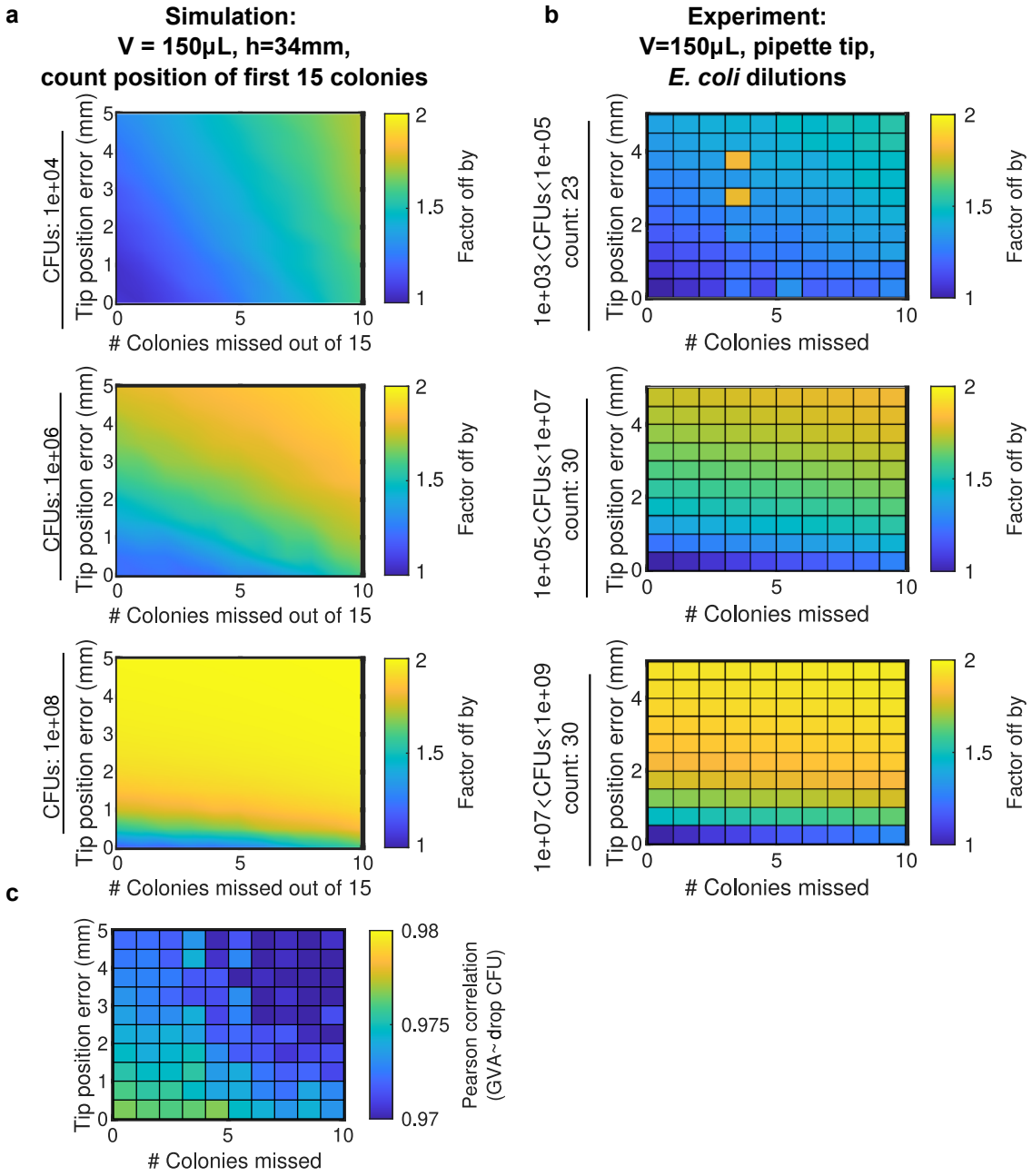

Figure S8: **Sensitivity analysis of GVA calculations to error in missing colonies and location of the tip.** a) Heatmap of the error as a function of both tip position and missing colony errors. b) Same analysis as in panel a, but with experimental data. CFUs/mL binned between 1e3 and 1e5 (top row), 1e5 and 1e7 (middle row), and 1e7 to 1e9 (bottom row). The number of pipette tips included in each bin is annotated by the count. c) Heatmap of the the Pearson correlation between the drop CFU and GVA for both tip position and missing colony errors.

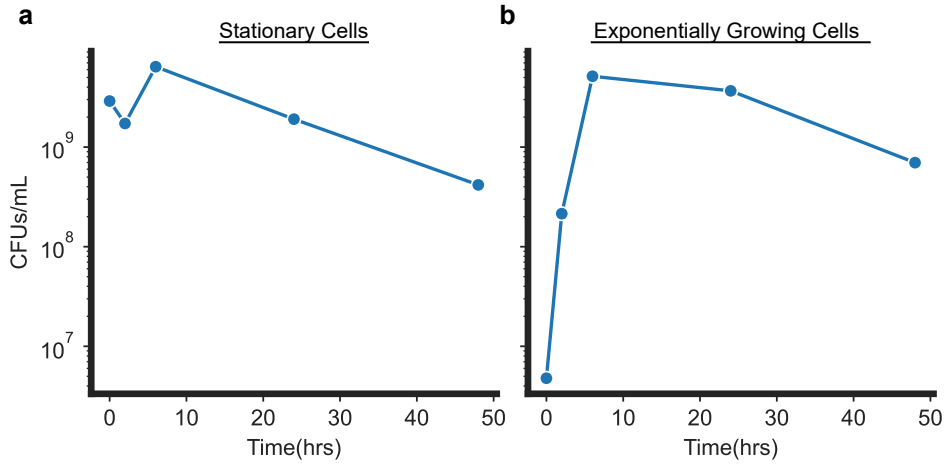

Figure S9: **Cell counts over time in stationary versus exponential cultures.** a) Number of CFUs/mL in stationary (a) versus exponential culture (b). To generate exponential culture, stationary phase cells were diluted 1:1000 in fresh LB media and place in the shaking incubator (180RPM) at 37 °C for 2 hours prior to beginning experiment.

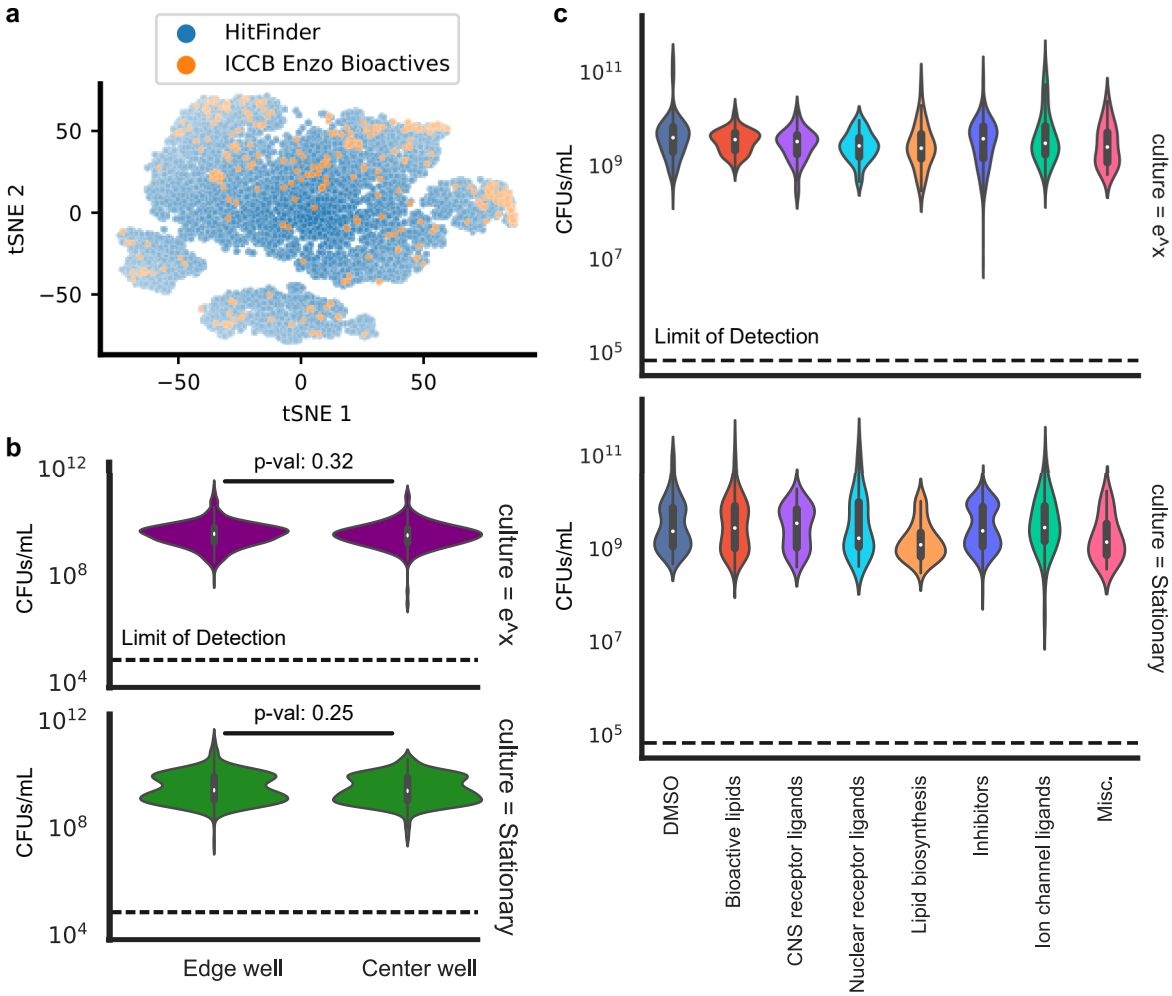

Figure S10: **Enzo screen controls.** a) Library diversity of ICCB Enzo Known Bioactive library compared to the Maybridge HitFinder library. Tanimoto similarity between all molecules based on SMILES was calculated using the RDKit package in python. From this distance matrix, the tSNE embedding was initialized with PCA and computed with a perplexity of 50. b) Distribution of CFUs/mL for conditions on the edge of the plate versus in the center wells for both stationary and exponential cultures. Statistical test used a Mann-Whitney U test for nonparametric distributions (p-val> 0.05). c) Distribution of CFUs/mL for different drug classes identified in the Enzo Library (See Fig. 5c). No class differences were found when using ANOVA (p-val>0.001, p-val corrected for multiple hypothesis testing). No differences from control were found using the Pairwise Tukey Test (p-val>0.01, Pairwise Tukey Test)

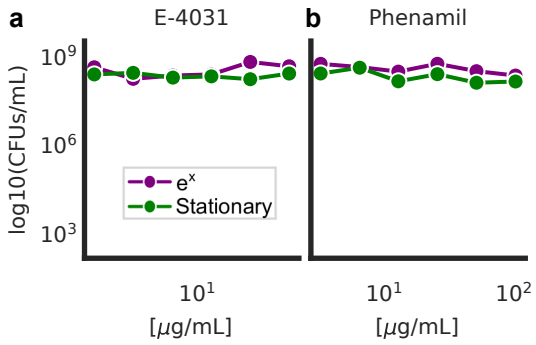

Figure S11: **Non-validated hits from the ICCB Enzo bioactive screen.** E-4031 (a) and phenamil (b) dose-response curves against stationary or exponentially (e^x) growing cultures.

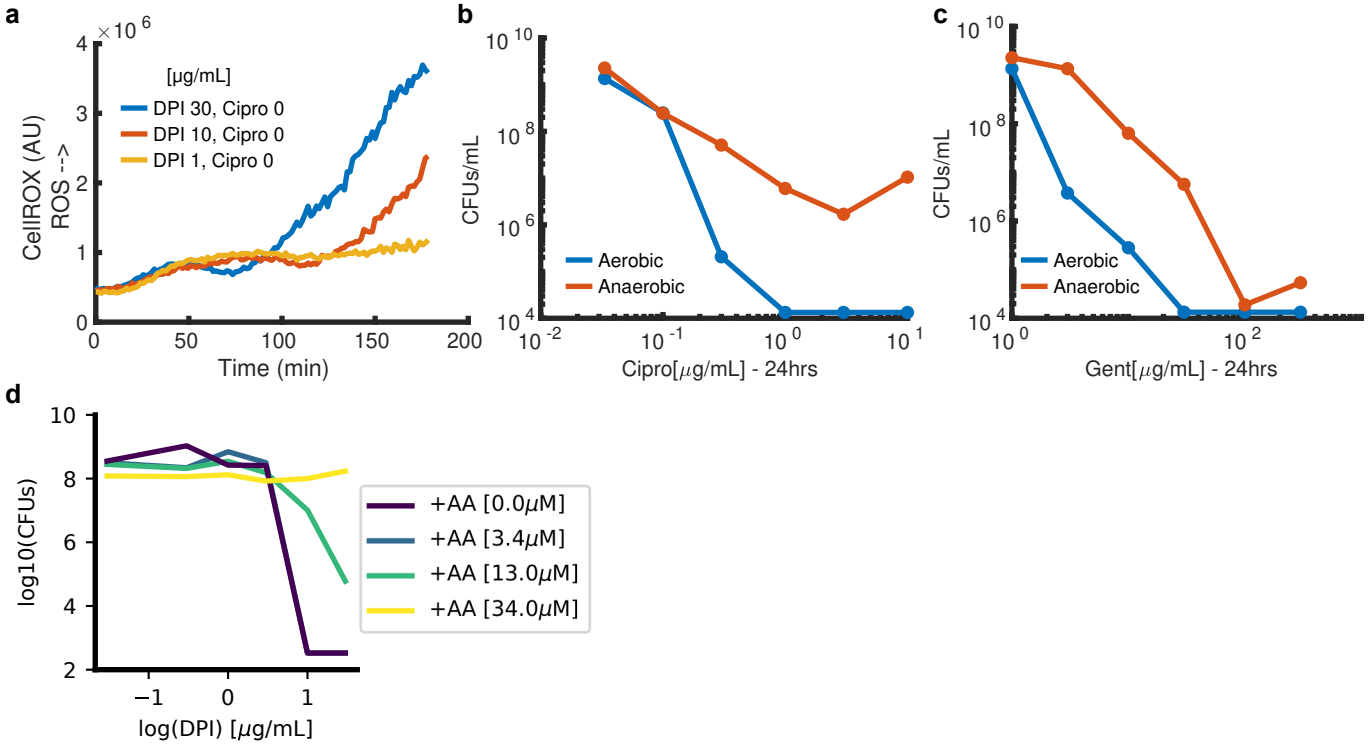

Figure S12: a) Duration of ROS reduction and onset of the secondary ROS spike is DPI-concentration dependent. Depicted is the median single-cell CellROX signal as a function of time for different concentrations of DPI. b,c) Dose response curve for ciprofloxacin (b) and gentamicin (c) against stationary phase cells in aerobic or anaerobic conditions. Treatment was for 24 hours. d) Efficacy of DPI as a function of increasing concentrations of the ROS-scavanger, ascorbic acid (AA).

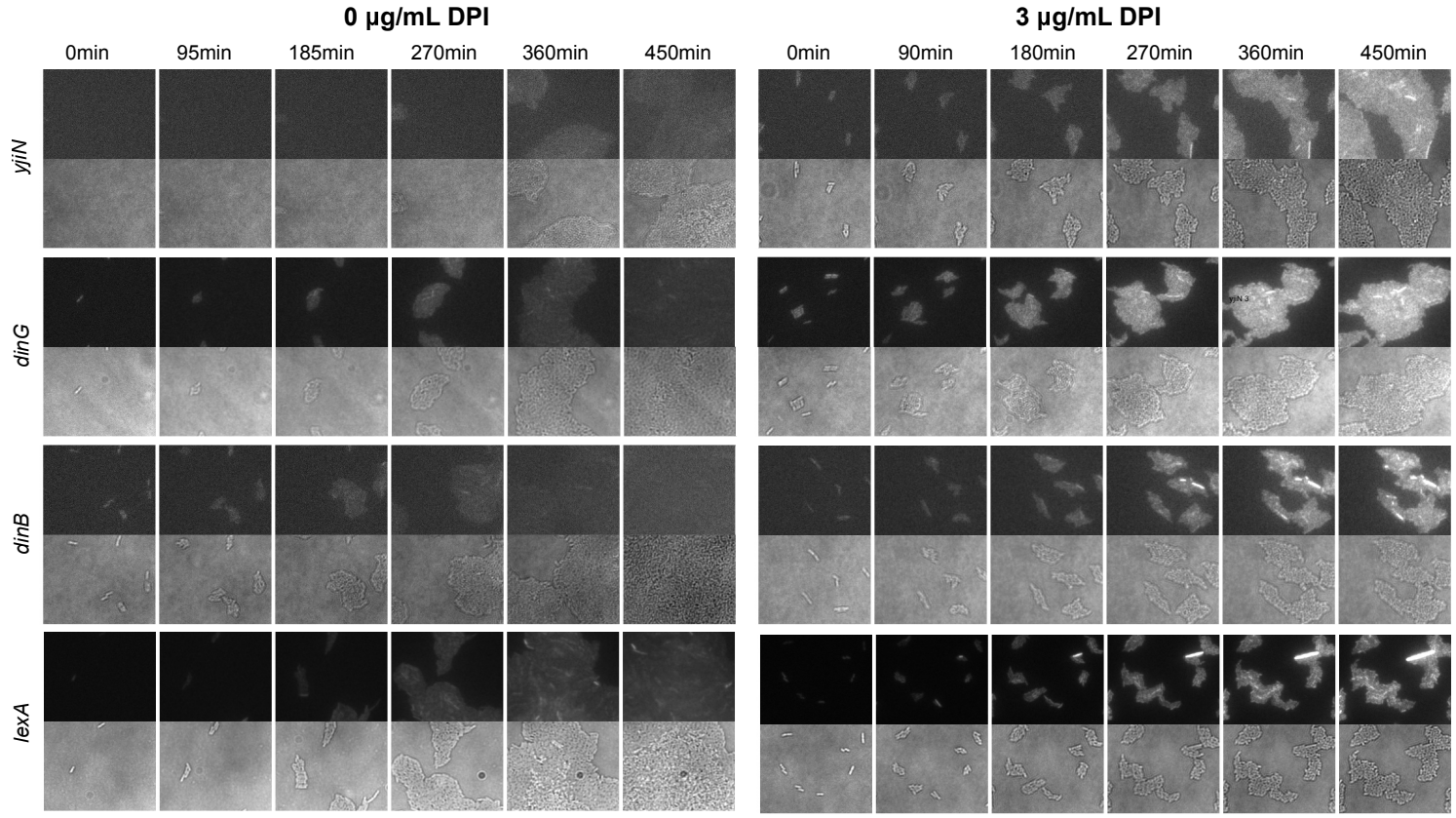

Figure S13: Strip charts of lexA-repressed genes (rows) using the PEC library. GFP fluorescence (top panels of each row) is proportional to each gene's promoter activity. Bottom panel of each row depicts brightfield image. Columns correspond to different timepoints post treatment.

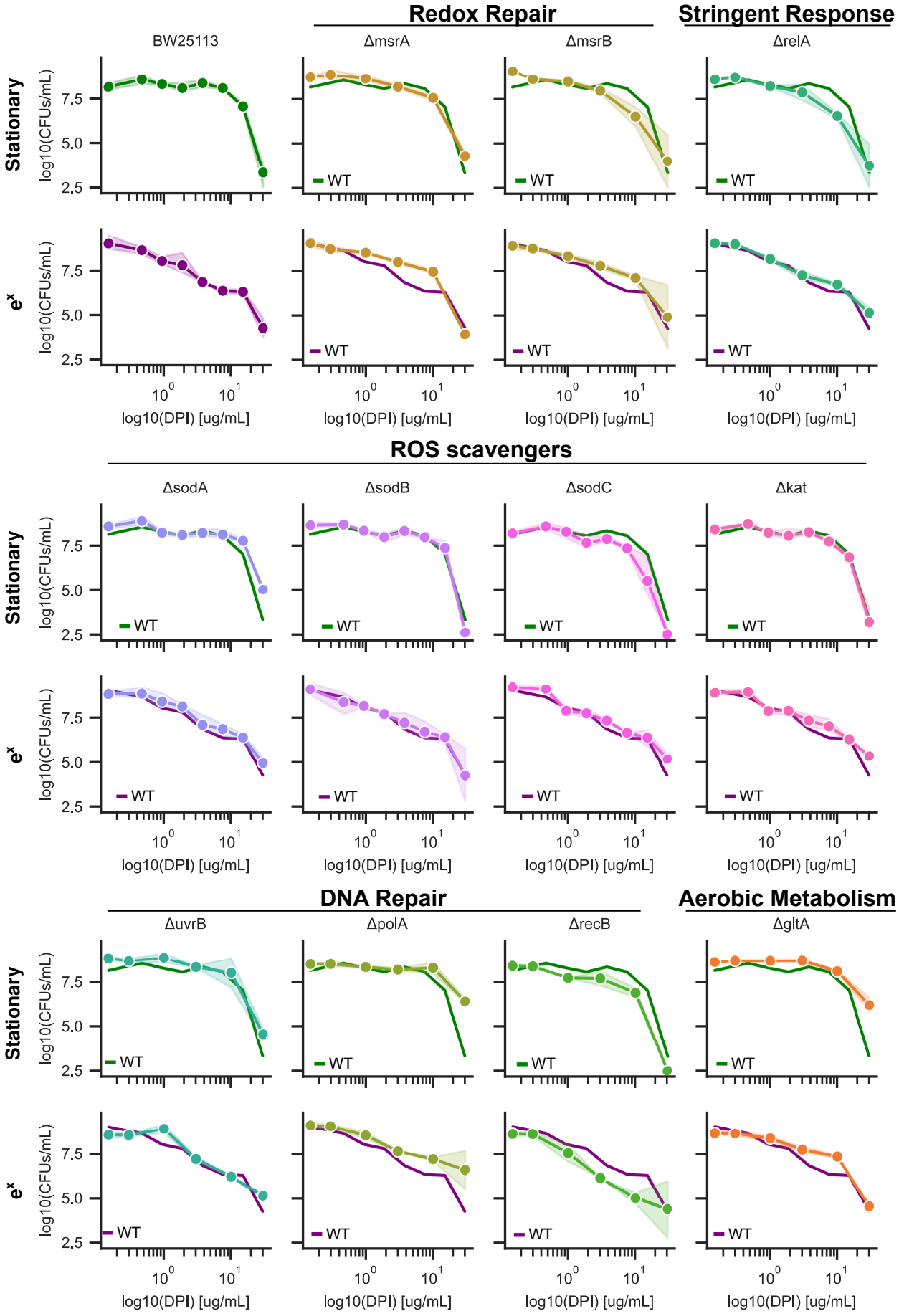

Figure S14: **Sensitivity of gene mutants to DPI in exponential and stationary phase.** Wild type reference depicted in solid line for each mutant. Error bars are the standard deviation in log space between three biological replicates. Mutants were selected from the Keio collection. Kanamycin (25 μg/mL) was included in the all Keio culture conditions both in the overnight culture and during treatment with DPI to maintain gene knockout.

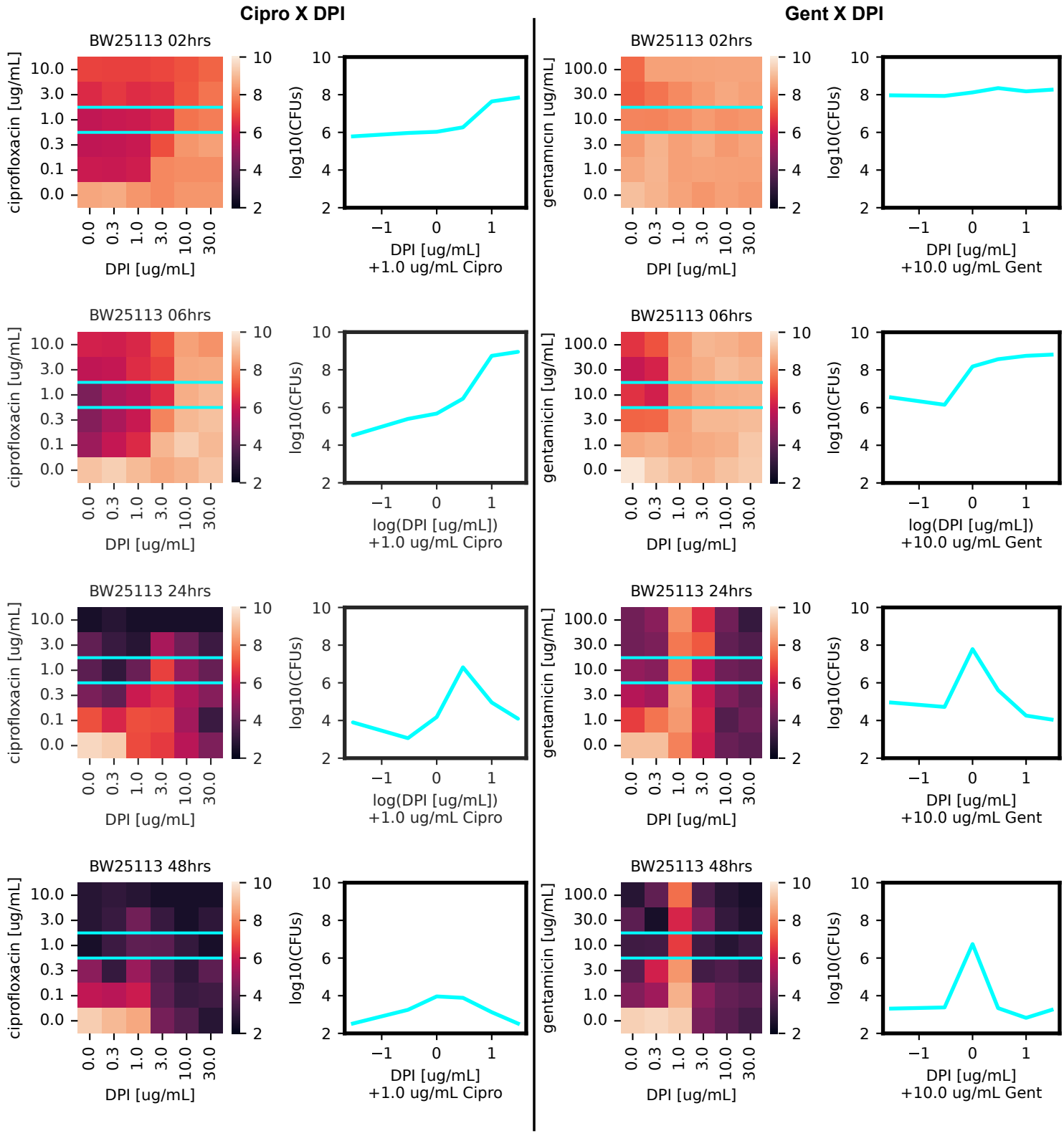

Figure S15: **GVA temporal checkerboard of DPI crossed with either ciprofloxacin (left panels) or gentamicin (right panels) against *E. coli*.** Treatment time increases down the rows. Each square in the heatmap was the mean of duplicate conditions. Colorbar correspond to the measured log10(CFUs/mL) for each combination. Left panel shows line trace (cyan) for the DPI dose response at 1μg/mL ciprofloxacin or 10 μg/mL gentamicin.

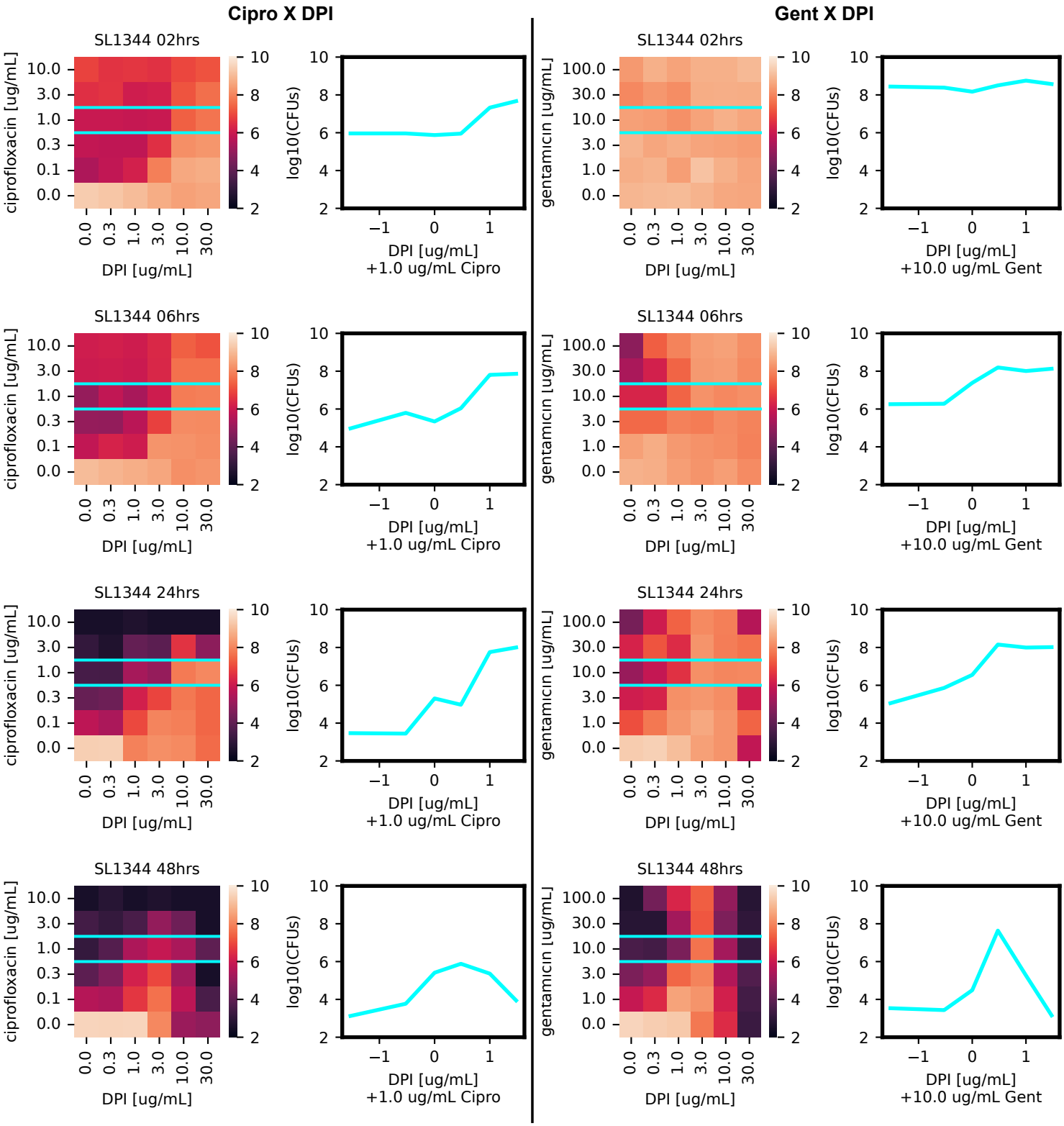

Figure S16: **GVA temporal checkerboard of DPI crossed with either ciprofloxacin (left panels) or gentamicin (right panels) against *S. typhimurium*.**

4 Derivation of the axial probability density function for a cone.

Assuming single cells are well mixed before being suspended and cast into a 3D cone, the probability of a colony forming at distance x from the origin is proportional to the percent of the total volume (V) comprised by the infinitesimal volume (dV) at x. dV is defined as

$$dV = \pi r'(x)^2 * dx \tag{3}$$

where $r'(x)$ is the radius of the circle at x (Fig. S1a, cyan circle). Based on the geometry in Fig. S1a (right panel), we find

$$r'(x) = \frac{r}{h} * x \tag{4}$$

where r is the radius of the cone's base and h is the height of the cone.

The probability density function (PDF) for this geometry can be solved for by

$$C * \int_0^h \frac{\pi r^2}{h^2} x^2 dx = 1 \tag{5}$$

where C is the normalization constant and is equal to the inverse of the the volume V (i.e. $C = \frac{3}{\pi h r^2}$) This leads to the following PDF (Fig. S1b)

$$PDF(x) = \frac{3 * x^2}{h^3} \tag{6}$$

The associated Cumulative Distribution Function (CDF) can be found from the integral (Fig. S1c)

$$CDF(x) = \frac{x^3}{h^3} \tag{7}$$

We can observe here that regardless of the base shape of the cone or pyramid, as long as it is axially symmetric, this PDF holds (Fig. S1d) as a result of the specific geometry of dV canceling out of the PDF due to the normalization constant. Following the same derivation, the PDF of a cylinder is found to be a constant $\frac{1}{h}$ and the PDF of a 2D wedge is $\frac{2*x}{h^2}$ (Fig. 1b). Because of the exponent on x, the PDF of the cone gives the largest dynamic range in the probability (Fig. 1b). The CDF measures the likelihood of having found a colony as function of x if only a single colony is in the cone (Fig. 1b). The PDF is the probability of finding a colony at any point x for only a single colony in the cone. Therefore, there are two equivalent ways of calculating the number of CFUs using either the PDF or the CDF (Fig. S1e).

With the PDF we can estimate the number of CFUs/mL using the equation

$$CFUs/mL = \frac{\#Colonies\ between\ x_1\ and\ x_2}{V * \int_{x_1}^{x_2} PDF(x)dx} \tag{8}$$

where x_1 and x_2 is the position of the first and last colony and V is the cone volume.

With the CDF,

$$CFUs/mL = \frac{\#Colonies\ between 0\ and\ x}{V * CDF(x)} \tag{9}$$

In practice, we find using the PDF estimator to be more convenient because it does not depend on identifying the first colony from the tip, but mathematically these are equivalent.